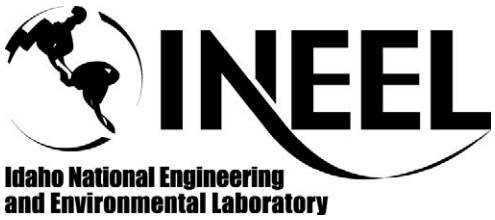

Idaho National Engineering
and Environmental Laboratory

INEEL/CON-04-01642
PREPRINT

Film Boiling On Downward Quenching Hemisphere Of Varying Sizes

Chan S. Kim – Seoul National University
Kune Y. Suh – Seoul National University
Joy L. Rempe – INEEL
Fan-Bill Cheung – The Pennsylvania State Univ.
Sang B. Kim – Korea Atomic Energy Research Institute

April 25 – 29, 2004

12th International Conference on Nuclear Engineering and 2004 ICAAP

Proceedings of ICONE12
12th International Conference on Nuclear Engineering
April 25-29, 2004, Arlington, Virginia, USA

ICONE12-49305

FILM BOILING ON DOWNWARD QUENCHING HEMISPHEREOF VARYING SIZES

Chan S. Kim, Kune Y. Suh*
Seoul National University
San 56-1 Sillim-dong, Gwanak-gu, Seoul, 151-742, Korea
*E-mail: kysuh@snu.ac.kr

Joy L. Rempe
Idaho National Engineering & Environmental Laboratory
P.O. Box 1625, Idaho Falls, ID 83415, USA
E-mail: yoj@inel.gov

Fan-Bill Cheung
Pennsylvania State University
304 Reber Building, University Park, PA 16802, USA
E-mail: fxc4@psu.edu

Sang B. Kim
Korea Atomic Energy Research Institute
P.O. Box 105, Yuseong, Taejon, 305-600, Korea
E-mail: sbkim2@kaeri.re.kr

ABSTRACT

Film boiling heat transfer coefficients for a downward-facing hemispherical surface are measured from the quenching tests in DELTA (Downward-boiling Experimental Laminar Transition Apparatus). Two test sections are made of copper to maintain low Biot numbers. The outer diameters of the hemispheres are 120 mm and 294 mm, respectively. The thickness of all the test sections is 30 mm. The effect of diameter on film boiling heat transfer is quantified utilizing results obtained from the test sections. The measured data are compared with the numerical predictions from laminar film boiling analysis. The measured heat transfer coefficients are found to be greater than those predicted by the conventional laminar flow theory on account of the interfacial wavy motion incurred by the Helmholtz instability. Incorporation of the wavy motion model considerably improves the agreement between the experimental and numerical results in terms of heat transfer coefficient. In addition, the interfacial wavy motion and the quenching process are visualized through a digital camera.

INTRODUCTION

In the design for the APR1400 (Advanced Power Reactor 1400 MWe), the concept of in-vessel retention through external vessel cooling (IVR-EVC) was chosen as a severe accident management strategy. The cavity flooding was selected as the external vessel cooling method because of simpler installation relative to flooding within the thermal insulator. In fact, the IVR-EVC concept had not been considered during the initial design phase of the APR1400. Thus, several issues surfaced while applying the IVR concept at a later stage of design. One of these issues centered about delayed flooding of the reactor vessel because of the large volume between the cavity floor and the lower head. The cavity flooding and flooding within the thermal insulator may take as much as forty minutes depending upon the accident scenario. It is thus not certain whether the flooding time will always be shorter than the time for relocation of the molten core material to the lower plenum of the reactor vessel. In addition, the initial temperature of the vessel will far exceed the cavity flooding water temperature in the vicinity of the saturation temperature corresponding to the primary system pressure during an accident. Hence, the initial heat removal mechanism for external vessel cooling will most likely be film rather than nucleate boiling. It turned out, however, that film boiling heat transfer coefficients presently available in the literature tend to underpredict the actual value for the reactor vessel lower head.

Bromley [1], Koh [2], Sparrow and Cess [3], and Nishikawa and Ito [4] investigated film boiling on vertical plates. They applied the various boundary conditions to prediction of film boiling heat transfer coefficients. Generally, the boundary conditions at the interface between the vapor film and bulk liquid were divided into zero interfacial velocity and the same interfacial shear stress. Frederking and Clark [5], Sakurai et al. [6], and Tou and Tso [7] studied models for the laminar film boiling heat transfer coefficients on spheres based on the previous analytic solutions for those on the vertical plates.

Experimentally-measured film boiling heat transfer coefficients were higher for a relatively long vertical plate than those predicted for the laminar film boiling [8]. Dhir and Purohit [9] measured film boiling heat transfer coefficients 50~60 % higher than those predicted by the laminar plane interface theory for spheres. Kolev [10] developed the correlation with the Helmholtz instability at vertical plates and spheres. Kim [11] performed experiments with nickel-plated copper spheres of various diameters to study film boiling heat transfer and its stability in flowing water. Experimental data are nonexistent for the downward-facing hemisphere on a large scale, however.

In this study, film boiling heat transfer coefficients are obtained from the quenching test DELTA (Downward-boiling Experimental Laminar Transition Apparatus) utilizing the measured temperature-time histories. The quenching processes are visualized through a digital camera.

NOMENCLATURE

Bi	Biot number
c_p	specific heat of test section
$c_{p,v}$	specific heat of vapor
D	diameter of test section
G	ratio of volume to outer area of test section
g	gravitational acceleration
h_{film}	film boiling heat transfer coefficient
h_{lv}	latent heat of water
h^*_{lv}	effective latent heat of water
h_{rad}	radiation heat transfer coefficient
Ja	Jacob number
k	thermal conductivity of copper
k_v	thermal conductivity of vapor
Nu	Nusselt number $Nu = h_{film} D / k_v$
R	radius of test section
r	radial component in spherical coordinate
Ra	Rayleigh number
Re_δ	vapor film Reynolds number
T	temperature
T_w	wall temperature
U_{hfilm}	uncertainty in film boiling heat transfer coefficient
U_T	uncertainty in average temperature in test section
u	azimuthal velocity
u_δ	interfacial velocity
w_i	interfacial mass flow rate
w_l	interfacial mass flow rate of liquid
w_v	interfacial mass flow rate of vapor

Greek Letters

α_v	thermal diffusivity of vapor
ΔT	temperature differential during time step
Δt	time step size
ΔT_{sup}	wall superheat
δ	vapor film thickness
μ_v	viscosity of vapor
θ	angular component in spherical coordinate
ρ	density of test section
ρ_l	density of liquid
ρ_v	density of vapor
τ_i	interfacial shear stress
τ_l	interfacial shear stress of liquid
τ_v	interfacial shear stress of vapor

LAMINAR FILM BOILING

The assumptions adopted in this analysis include the incompressible flow model, the Boussinesq approximation, negligible inertia and convection terms, the laminar film layer, fluid motion in the boundary layer only, the temperature-independent vapor thermodynamic properties, negligible viscous heating, stable and thin film layer, smooth wall surface, and negligible effect of the interfacial wave. The assumptions and simplifications used by Tou and Tso [7] were adopted in this analysis. General boundary conditions for laminar film boiling were applied. Figure 1 presents the schematic diagram of laminar film boiling from a downward-facing hemisphere. Especially, the two interfacial velocity boundary conditions were applied. Case 1 assumes that the interfacial velocity is zero. Case 2 presumes that the interfacial shear stress has the same value in vapor film and bulk liquid, and that the value is small enough to be neglected. Vapor properties are evaluated at the film temperature. The actual laminar film boiling heat transfer coefficient lies between the two cases [7]. Table 1 shows the calculated process for the laminar film boiling heat transfer coefficient for these two cases.

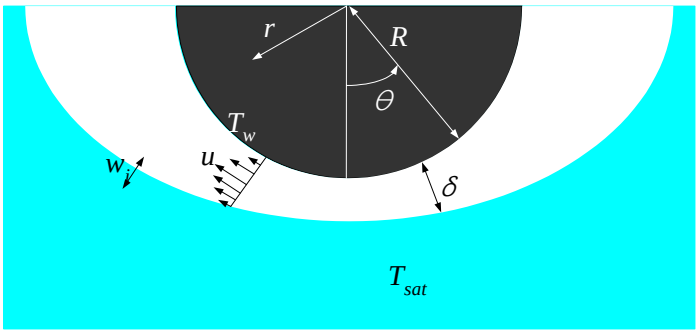

Figure 1. Laminar Film Boiling from a Downward-facing Hemisphere

INTERFACIAL WAVY MOTION IN FILM BOILING

Hsu and Westwater [12] estimated the condition for the onset of transition to turbulent flow in film boiling as

$$\mathrm{Re}_\delta = \frac{\rho_v u_\delta \delta}{\mu_v} = 100 \qquad (1)$$

With increasing angle starting from the bottom, the vapor film continues to thicken, and the vapor flow becomes more

turbulent. The interfacial waves accordingly increase in wavelength, eventually becoming unstable. When this occurs, the interfacial waves may roll up and break releasing vapor bubbles into the adjacent liquid. Thus, the vapor film developed from the transition position again. It was assumed that the onset of transition to turbulent flow in film boiling occurred, when the vapor film Reynolds number is 78. The angular vapor film thickness and interfacial velocity were calculated under the boundary conditions of case 2 as illustrated in Figure 2 accounting for the interfacial wavy motion.

Table 1 Process of Numerical Analysis

Governing Equations		$\frac{\partial}{\partial\theta}(u\sin\theta)=0 \quad \frac{\mu}{r^2}\frac{\partial}{\partial r}\left(r^2\frac{\partial u}{\partial r}\right)=g(\rho_l-\rho_v)\sin\theta \quad \frac{1}{r^2}\frac{\partial}{\partial r}\left(r^2\frac{\partial T}{\partial r}\right)=0$
Boundary Conditions		$r=R \rightarrow u=0,\ T=T_w \qquad -k\frac{\partial T}{\partial r}2\pi R^2\sin\theta=h_{fg}dw_i$
		$r=R+\delta \rightarrow T=T_{sat} \qquad dw_v=dw_i=d\left(\int_R^{R+\delta}\rho u\,2\pi R\sin\theta dr\right)$ $u=0 \ \text{or} \ \tau_i=\tau_l=\tau_v=-\mu\frac{\partial u}{\partial r}=0$
Temperature Profile		$\frac{T-T_s}{T_w-T_s}=1+\frac{r^{-1}-R^{-1}}{R^{-1}-(R+\delta)^{-1}} \qquad \left(\frac{dT}{dr}\right)_{r=R}=-\frac{\Delta T}{\delta}\left(1+\frac{\delta}{R}\right)=-\frac{\Delta T}{\delta}$
Velocity Profile	***zero velocity***	$u=\frac{-g(\rho_l-\rho_v)\sin\theta}{6\mu_v}\left[r^2+\frac{2R^3+3R^2\delta+R\delta^2}{r}-3R^2-3R\delta-\delta^2\right]$
	same interfacial τ	$u=\frac{-g(\rho_l-\rho_v)\sin\theta}{3\mu_v}\left[\frac{r^2}{2}+\frac{(R+\delta)^3}{r}-\frac{R^2}{2}-\frac{(R+\delta)^3}{R}\right]$
Interfacial Mass Flow Rate	***zero velocity***	$dw_i=\frac{2\pi RRak_v}{96c_p}d\left[\sin^2\theta\left(\frac{\delta}{R}\right)^3\right]$
	same interfacial τ	$dw_i=\frac{2\pi RRak_v}{24c_p}d\left[\sin^2\theta\left(\frac{\delta}{R}\right)^3\right]$
Angular Film Thickness Distribution	***zero velocity***	$\frac{\delta}{R\left(1+\frac{\delta}{R}\right)}\frac{d}{d\theta}\left[\sin^2\theta\left(\frac{\delta}{R}\right)^3\right]=96\frac{Ja}{Ra}\sin\theta$
	same interfacial τ	$\frac{\delta}{R\left(1+\frac{\delta}{R}\right)}\frac{d}{d\theta}\left[\sin^2\theta\left(\frac{\delta}{R}\right)^3\right]=24\frac{Ja}{Ra}\sin\theta$
Final Results (Nu)	***zero velocity***	$Nu=0.696\left(\frac{Ra}{Ja}\right)^{0.25}+1$
	same interfacial τ	$Nu=0.985\left(\frac{Ra}{Ja}\right)^{0.25}+1$

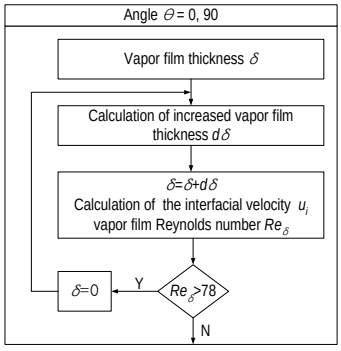

Figure 2. Calculation Process of Vapor Film Thickness

EXPERIMENTAL SETUP & DATA REDUCTION

Figure 3 presents the cross-sectional view of the test sections with diameters of 120 mm and 294 mm, respectively. The diameters of the stainless steel and Fire Stop disk on the test section respectively are 118 mm and 292 mm, which are smaller than the diameters of the two copper hemispheres. This explains why difference in thermal expansion of the three different materials does not interfere with release of bubbles on the top of the hemispheres. Figure 4 shows the thermocouples installed at 0°, 20°, 40°, 60° and 80° near the outer surface and the inner surface of both test sections. The thermocouples were calibrated in ISOTECH TRU (Temperature Reference Unit) Model 740. The holes were drilled through the center of the stainless steel disk, stainless steel pipe, and the Fire Stop to route the wall thermocouples to the HP-VXI E1413C data acquisition system. The test section is made of copper to maintain Bi below 0.1 in the film boiling regime. In case of Bi less than 0.1 the conduction heat transfer in the solid may be neglected [13]. Thus, the experimental data could be compared with numerical analysis for the isothermal hemispherical surface. The thickness of the copper vessel was 3 cm so that data from the quenching experiment would be obtained from similar structures as were used in the steady state experiment [14]. If the time to traverse the top 10 % of the boiling curve were greater than 1 sec, the boiling process would be in a quasi-steady state [15]. The test section's inner cavity was filled with bulk fiber and covered on top with the Fire Stop disk for thermal insulation. A stainless steel disk was fastened to the test section wall using the stainless steel bolts.

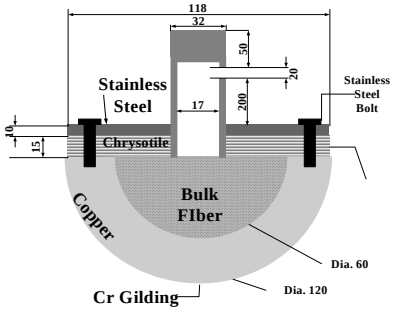

(a) 120 mm

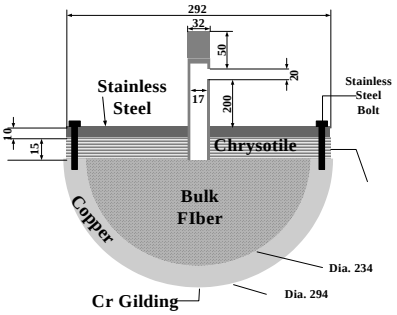

(b) 294 mm

Figure 3. Cross-section View of Test Sections

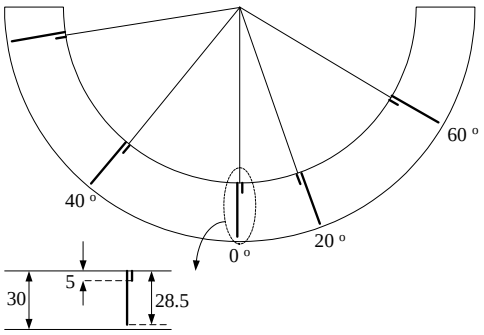

Figure 4. Azimuthal Locations of Thermocouples (length unit: mm)

The hexahedral quenching tank is of 1×1×1.1 m. A tank must have 3.5 times the dimension of the test section to maintain pool boiling without the effect of the quenching tank size [16]. It has a large glass window on one side for visual inspection and recording of pool boiling on the hemispherical surface during quenching using a video camera. During the experiment, the water in the tank was maintained at the saturated condition utilizing four 10 kW and two 7 kW heaters.

Prior to each quenching experiment, the demineralized water in the tank was degassed by boiling for thirty minutes. The test section was heated up to 280°C. The heated test section was transferred from the furnace to the quenching tank by an automatic lift for a few seconds. The heated test section was then submerged in the quenching tank with its top surface kept 10 cm below the water level. Figure 5 shows the experimental apparatus DELTA.

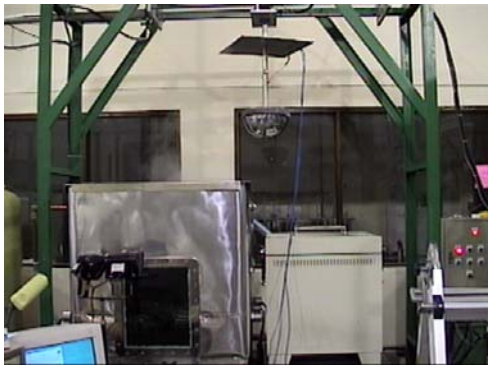

Figure 5. Picture of DELTA Apparatus

This experiment was designed to measure the temperature profile associated with the film boiling heat transfer coefficient. Measured temperature history was smoothed by means of a 10 point FFT-filter in Microcal Origin 6.0. The film boiling heat transfer coefficient was computed from the temperature history as follows

$$h_{film} = \frac{\rho c_p G \Delta T}{\Delta t \Delta T_{sat}} - 0.75 h_{rad} \qquad (2)$$

Pursuant to Equation (2), the heat transfer coefficient is determined by the wall temperature rate of change during the time step, wall superheat, and a geometrical parameter as well as material properties. The local temperature difference is small such that the conduction heat transfer can be neglected in the test sections so as to minimize uncertainties in the estimated film boiling heat transfer coefficients.

$$\frac{U_{hfilm}}{h_{film}} = \frac{\sqrt{2}U_T}{\Delta T} \qquad (3)$$

RESULTS AND DISCUSSION

In the experiments, the local temperature difference was found to stay within ± 0.5°C in the film boiling regime, because the thermal conductivity of the test sections was high. Hence, the conduction heat transfer could be neglected in obtaining the film boiling heat transfer coefficient. The average standard deviation of the film boiling heat transfer coefficient was ± 8 %.

Figure 6 shows the film boiling heat transfer coefficients with the wall superheat for diameter 120 mm resulting from the numerical analysis. The heat transfer coefficients from the experiments lie within the bounding values for cases 1 and 2. The film boiling regime for diameter 120 mm is laminar, but the heat transfer coefficients are closer to those for case 2. There is no difference between case 2 and the interface wavy motion.

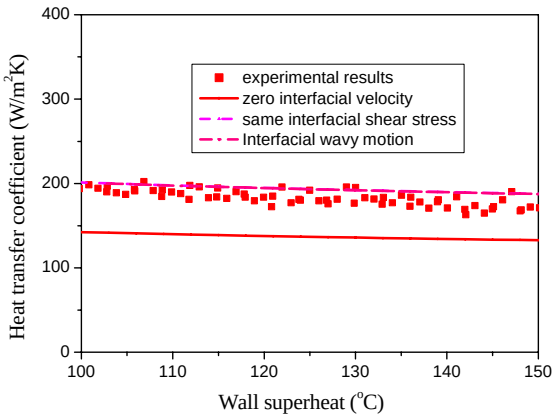

Figure 6. Film Boiling Heat Transfer Coefficient for Test Section of Diameter 120 mm

Figure 7 depicts the film boiling heat transfer coefficients varying with the wall superheat measured from diameter 294 mm and predicted by the numerical analysis. The heat transfer coefficients obtained from the tests are greater than those from the numerical analysis for case 2. Thus, the film boiling regime in the DELTA experiment is not simply laminar, but rather involves more complexities like the Helmholtz instability. The film boiling heat transfer coefficients considering the interfacial

wavy motion agree better with the experimental results than those for cases 1 and 2.

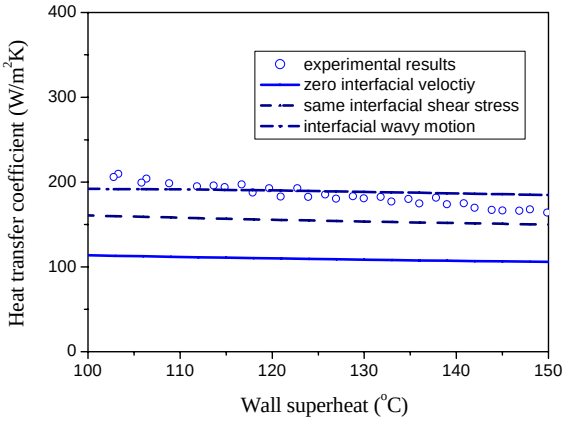

Figure 7. Film Boiling Heat Transfer Coefficient for Test Section of Diameter 294 mm

Figure 8 presents the vapor film Re for the conditions in the DELTA tests. For the test section with diameter 120 mm, the vapor film Re is always less than 78. Thus, the experimental data lie within the bounding values for cases 1 and 2. The transition angle when the vapor film Re reaches 78 lies in the vicinity of 60° for the test section with diameter 294 mm. Note that the larger the wall superheat, the less the transition angle. It turns out, however, that the measured data are underpredicted despite the large transition angle expected for the lower wall superheat in this test. According to Bui and Dhir [8], and Kolev [10], the interfacial wavy motion due to the Helmholtz instability is believed to be the key factor in explaining underprediction of the experimental results by the laminar film boiling analysis. The limiting vapor film thickness imposed by the Helmholtz instability will tend to increase the film boiling heat transfer due to local breakup of the film.

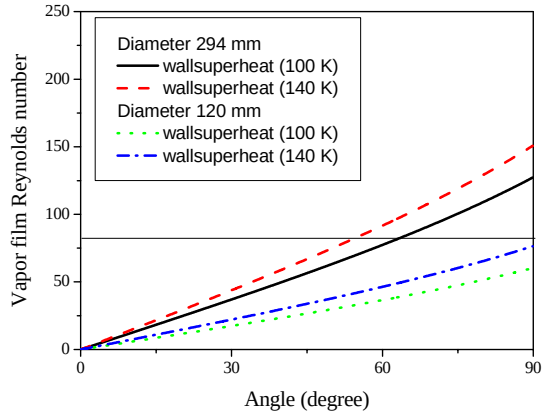

Figure 8. Vapor Film Reynolds Number for Test Sections at Laminar Film Boiling

Figure 9 compares the experimental results for the two test sections showing little difference in-between. It is surmised that similar film boiling heat transfer coefficients result from similar vapor film thickness in the two experiments. It is considered that the Helmholtz instability places limits on the vapor velocity and film thickness.

For a wall superheat of 120 K, the heat transfer coefficients obtained from the two diameters are plotted in Figure 10. The experimental data and the film boiling heat transfer coefficients with the interfacial wavy motion reveal little dependence of the heat transfer coefficient on the diameter. In contrast, the laminar film boiling heat transfer analysis predicts a monotonous reduction in the heat transfer with diameter. For the diameter of 120 mm, the heat transfer coefficient lies within the bounding values for cases 1 and 2 based on the laminar film boiling heat transfer.

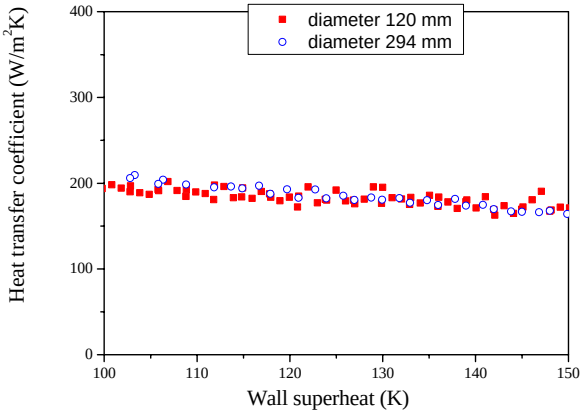

Figure 9. Comparison of Two Experimental Results

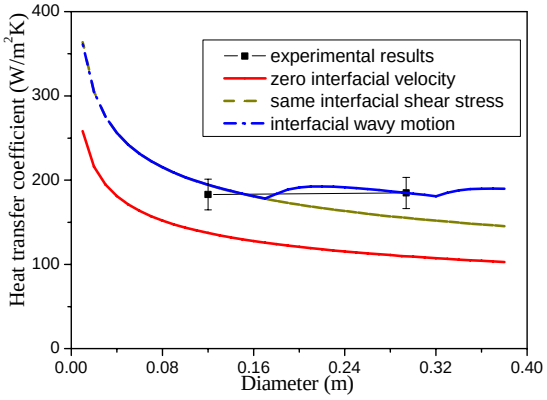

Figure 10. Comparison of Predicted and Observed Dependence of Heat Transfer Coefficient on Diameter of a Downward-facing Hemisphere

Figure 11 compares El-Genk and Glebov's experimental results [17] and the laminar film boiling analysis corresponding to their experimental condition. Spanning the whole range of wall superheat, their experimental data lie within the bounding

values of cases 1 and 2. The graph indicates that the film boiling regime was indeed laminar in their experiments.

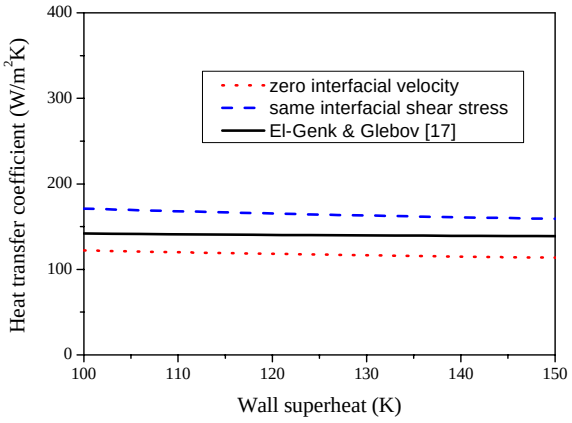

Figure 11. Comparison of Laminar Film Boiling Heat Transfer and El-Genk and Glebov's [17] Experiments

Figure 12 presents the film boiling heat transfer coefficients derived from the two experiments. The diameter of the test section in our experiments is the same as the curvature diameter of the test section in El-Genk and Glebov [17]. However, their test section was not a full downward-facing hemisphere, but rather a bottom piece whose edge angle was 9.88°. Both test sections are made of copper. The film boiling heat transfer coefficients from our experiments are larger than those from El-Genk and Glebov's experiments [17]. If the film boiling regime were strictly laminar in our experiments, the heat transfer coefficients should have been smaller than those from their experiment. This is because their test section covered only a limited lower portion of the hemisphere, whereas our test section represented the full hemisphere so that the thickening vapor film on the upper portion of the test section must have contributed to deteriorating heat transfer from our test section. It is thence speculated that the film boiling regime for diameter of 294 mm is not simply laminar. Most presumably, the interfacial wavy motion plays a pivotal role in augmenting heat transfer from the full hemisphere. In addition, the large edge angle increases the vapor removal on the edge. Hence, the large edge angle is seen to increase the film boiling heat transfer coefficients.

Figures 13 (a) and (b) depict the film boiling heat transfer mechanism for the two DELTA test sections. Snapshots were taken of film boiling with the digital camera Nikon D100 at 1000 fps. Considering the measured film boiling heat transfer coefficients, the governing mechanism was laminar film boiling. Thus, a relatively stable vapor film was formed on the 120 mm diameter downward-facing hemisphere. In case of diameter 294 mm, Figure 13 (b) reveals a rough vapor film interface on most of the downward-facing hemisphere. This had already been anticipated from the calculated heat transfer coefficients taking account of the interfacial wavy motion. A similar vapor film instability as had already been reported by Bui & Dhir [8] on the vertical plate was observed on most of the downward-facing hemisphere. The wavelength by the Helmholtz instability will quantitatively be analyzed in the visualization tests.

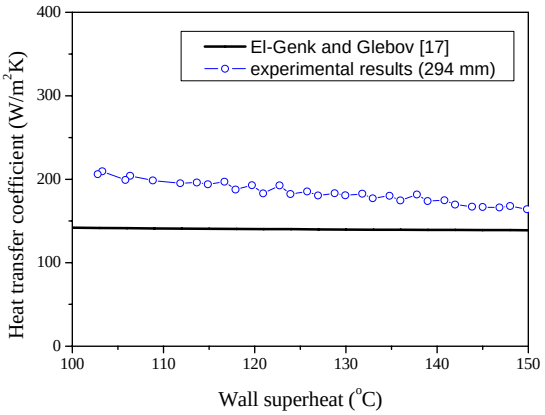

Figure 12. Comparison of Experimental Data for Test Section of Diameter 294 mm

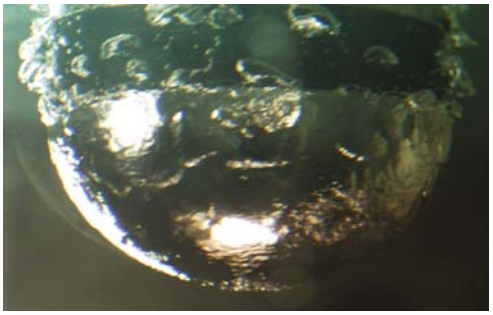

(a) 120 mm

(b) 294 mm

Figure 13. Film Boiling for Two Test Sections

Figures 14 (a) to (e) illustrate the quenching process on the downward-facing hemisphere of diameter 120 mm. Snapshots were taken from the video file by the digital video camera at 30 fps. Figure 14 (a) shows that the hemispherical surface was covered with a thin vapor film. The unstable vapor film was observed at the top. Figure 14 (b) presents that the surface

rewetting occurred first at the lowermost position. Figure 14 (c) demonstrates that the surface rewetting propagated radially outward. This corresponds to the transition boiling regime. The relatively small bubbles were observed to emerge on the hemispherical surface. The boiling mechanism captured in Figure 14 (d) is the nucleate boiling at the high heat flux condition near the critical heat flux (CHF). Large bubbles were violently generated from the heated surface. Figure 14 (e) illustrates the nucleate boiling in the low heat flux condition.

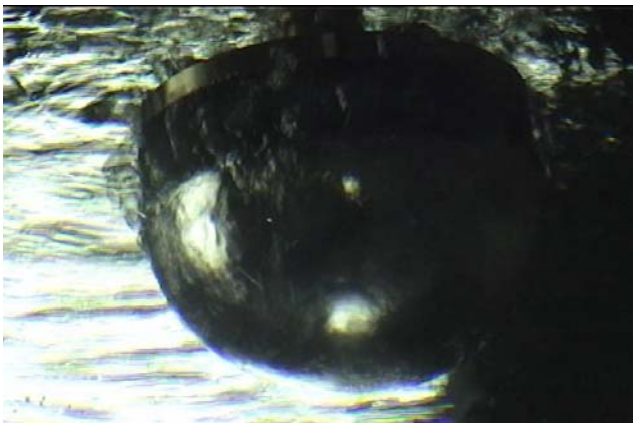

(a) Film Boiling

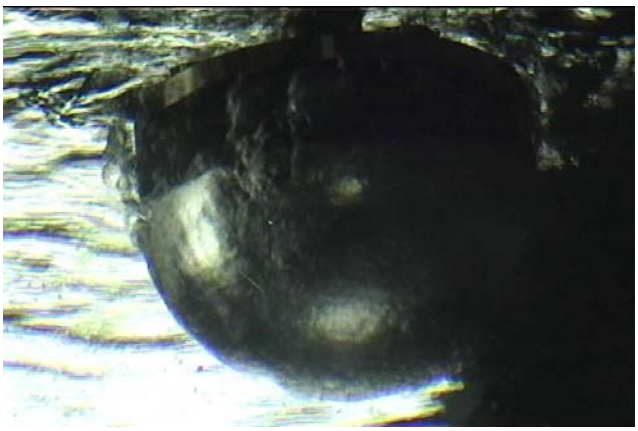

(b) Transition Boiling (Beginning of Surface Rewetting)

(c) Transition Boiling (Propagation of Surface Rewetting)

(d) Nucleate Boiling (High Heat Flux Condition)

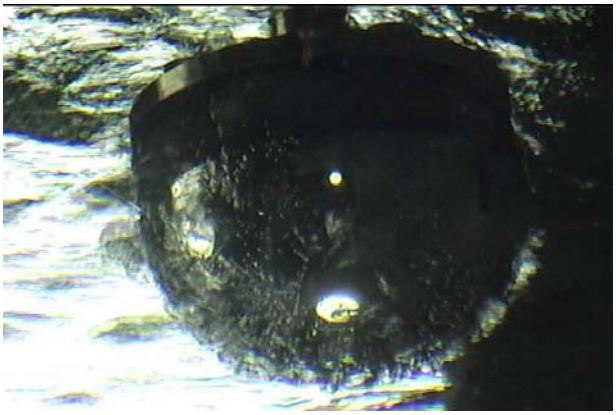

(e) Nucleate Boiling (Low Heat Flux Condition)

Figure 14. Quenching Process (120 mm)

Figures 15 (a) to (g) snapshot the quenching process on the downward-facing hemisphere with diameter 294 mm. Figure 15 (a) shows that the hemispherical surface was covered with the unstable vapor film. The larger diameter facilitates detailed visualization of the surface rewetting propagation. Figures 15 (b) and (c) indicate that the surface rewetting propagated radially inward. According to visual observation, destabilization of film boiling propagated radially outward for the downward-facing hemisphere of diameter 120 mm. On the other hand, destabilization spread radially inward for the downward-facing hemisphere of diameter 294 mm. This is due to the difference in the minimum film thickness location between the two test sections. For the 120 mm test section, the location is 0°. However, the interfacial wavy motion due to the Helmholtz instability thins out the vapor film in the upper region for the 294 mm test section. This in turn results in the different starting points for the film boiling collapse. Figures 15 (d) and (e) depict that the nucleate boiling regime also propagated radially inward. The boiling mechanism shot in Figure 15 (f) is nucleate boiling at the high heat flux condition near the CHF. Large bubbles are vigorously generated from the heated surface. Figure 15 (g) portrays the nucleate boiling regime when the vapor generation rate is relatively low.

(a) Film Boiling

(b) Transition Boiling

(c) Transition Boiling (Propagation of Surface Rewetting)

(d) Beginning of Nucleate Boiling

(e) Propagation of Nucleate Boiling

(f) Nucleate Boiling (High Heat Flux Condition)

(g) Nucleate Boiling (Low Heat Flux Condition)

Figure 15. Quenching Process (294 mm)

CONCLUSIONS

Film boiling heat transfer coefficients on the downward-facing hemisphere were measured and analyzed. Major results may be summarized as follows.

The film boiling regime for the test section of diameter 120 mm was laminar. The heat transfer coefficients were closer to those for the same interfacial shear stress boundary condition. On the other hand, the film boiling heat transfer coefficients for the test section of diameter 294 mm were greater than those given by the numerical solution for the laminar film boiling due mostly to the Helmholtz instability. There was little difference

observed between the film boiling heat transfer coefficients from the two test sections of diameters equal to 120 mm and 294 mm.

The interfacial wavy motion is considered to be the governing mechanism in determining the film boiling heat transfer coefficient in the test section with diameter 294 mm. Additionally, the large vertical edge angle in the full hemisphere used in our experiments increased the film boiling heat transfer coefficients relative to those from experiments using a lower segment of the hemisphere.

Destabilization of film boiling propagated radially inward for 294 mm, but radially outward for 120 mm.

Predictive correlations will be developed utilizing the test data from the hemispherical downward heated surface and flat inclined plates. Clear-cut visualization data will be produced to facilitate theorizing the film boiling on the curved surface.

ACKNOWLEDGMENTS

This work was performed under the auspices of the Ministry of Science and Technology, Korea and the Department of Energy, USA as part of the International Nuclear Energy Research Initiative program awarded to the Seoul National University and the Idaho National Engineering and Environmental Laboratory in collaboration with the Korea Atomic Energy Research Institute and the Pennsylvania State University.

REFERENCES

1. Bromely, L. A., 1950, “Heat Transfer in Stable Film Boiling,” Chemical Engineering Progress, **46**, pp. 221-227.

2. Koh, J. C., 1962, “Analysis of Film Boiling on Vertical Surfaces,” Journal of Heat Transfer, **84**, pp. 55-62.

3. Sparrow, E. M. and Cess, R. D., 1962, “The Effect of Subcooled Liquid on Laminar Film Boiling,” Journal of Heat Transfer, **84**, pp. 103-115.

4. Nishikawa, K. and Ito, T., 1966, "Two-Phase Boundary Layer of Free Convection Film Boiling," International Journal of Heat and Mass Transfer, **8**, pp. 103-115.

5. Frederking, T. H. and Clark, J. A., 1963, “Natural Convection Film Boiling on a Sphere,” Advanced Cryogenic Engineering, **8**, pp. 501-506.

6. Sakurai, A., Shiotsu, M. and Hata, K., 1990, “A General Correlation for Pool Film Boiling Heat Transfer from a Horizontal Cylinder to Subcooled Liquid: Part 1- A Theoretical Pool Film Boiling Heat Transfer Model Including Radiation Contribution and Its Analytical Solution,” Journal of Heat Transfer, **112**, pp. 430-440.

7. Tou, S. K. and Tso, C. P., 1997, “Improvement on the Modeling of Film Boiling on Spheres,” International Communication of Heat and Mass Transfer, **24**, 6, pp. 879-888.

8. Bui, T. D. and Dhir, V. K., 1985, “Film Boiling Heat Transfer on Vertical Plates and Spheres,” Journal of Heat Transfer, **107**, pp. 764-771.

9. Dhir, V. K. and Purohit, G. P., 1978, “Subcooled Film Boiling Heat Transfer from Spheres,” Nuclear Engineering and Design, **47**, pp. 49-66.

10. Kolev, N. I., 1998 “Film Boiling on Vertical Plates and Spheres,” Experimental Thermal and Fluid Science, **18**, pp. 97-115.

11. Kim, J. H., 1994, "Film Boiling Stability and Heat Transfer on Spheres," Ph.D. Thesis, University of Manchester, England.

12. Hsu, Y. Y. and Westwater, J. W., 1960, “Approximate Theory for Film Boiling on Vertical Surfaces,” Chem. Engr. Prog. Symp. Ser., **56**, 30, pp. 15-24.

13. Incropera, F. P. and Dewitt, D. P., 1996, *Introduction to Heat Transfer*, 3rd ed., Ch. 5, John Wiley and Sons, Inc., New York, NY, USA.

14. Peyayopanakul, W. J. and Westwater, W., 1978 “Evaluation of the Unsteady-state Quenching Method for Determining Boiling Curves,” International Journal of Heat and Mass Transfer, **21**, pp. 1437-1445.

15. Dhir, V. K., 1998 “Boiling Heat Transfer,” Annual Review of Fluid Mechanics, **30**, pp. 365-401.

16. Westwater, J. W., Hwalek, J. J., Irving, M. E., 1986, “Suggested Standard Boiling Curves by Quenching,” Ind. Eng. Chem. Fundam., **25**, pp. 685-692.

17. El-Genk, M. S. and Glebov, A. G., 1995, “Film Boiling from a Downward-Facing Curved Surface in Saturated and Subcooled Water,” International Journal of Heat and Mass Transfer, **39**, 2, pp. 275-288.

18. El-Genk, M. S. and Gao, S., 1999, “Experiments on Pool Boiling of Water from Downward-Facing Hemisphere,” Nuclear Technology, **125**, pp. 52-69.

19. Cheung, F. B., Haddad K. H., and Liu, Y. C., 1997 “Critical Heat Flux Phenomenon on a Downward Facing Curved Surface,” NUREG/CR-6507 PSU/ME-7321, Pennsylvania State University, University Park, PA, USA.

